Journal of Fluids and Structures 17 (2003) 97–113

JOURNAL OF FLUIDS AND STRUCTURES

www.elsevier.nl/locate/jnlabr/yjfls

Flow/acoustic interactions of two cylinders in cross-flow

J.A. Fitzpatrick

Department of Mechanical Engineering, Parsons Building, Trinity College, Dublin 2, Ireland

Received 15 November 2000; accepted 16 December 2001

Abstract

The noise generated by two tandem cylinders in a cross-flow (i.e., with the second in the wake of the first) has been investigated. Measurements of turbulence and of fluctuating pressure have been obtained between the two cylinders for different flow velocities and incident levels of turbulence. Although, for a number of cases, up to four peaks related to vortex shedding were evident in the spectrum, most measurements exhibited two peaks, a dominant one at the vortex-shedding frequency, with a secondary peak at twice this value. The measurements show that vortex generated noise is strongest at the mid-point between the cylinders and at the rear cylinder with levels of 130 dB. The harmonic component was strongest at the downstream cylinder where peak values of 110 dB were obtained. The nonlinear flow/acoustic interactions are examined using bispectral analysis to identify the quadratic interactions in the parameters. A novel quadratic modelling method is proposed and shown to be capable of both identifying and quantifying the nonlinear interactions which give rise to noise at harmonics of the vortex-shedding frequency.

1. Introduction

The generation of noise by flow over solid bodies is of interest in a number of engineering applications. For example, the reduction of noise from aero engines has resulted in an increased focus on the noise generated by the airframe structure, particularly undercarriage components. In general, the capacity for the prediction of noise generated by simple configurations such as two cylinders in cross-flow is limited, as the mechanisms of noise production are poorly understood. Although the noise generated by arrays of cylinders in cross-flow has been investigated by numerous authors [e.g., Ziada and Oengören (1989), Belvins and Bressler (1987), Fitzpatrick (1985)], there has been little reported on the noise emanating from smaller groups of cylinders, particularly in unbounded flows. The noise generated by a single cylinder has been investigated by numerous authors since the empirical work of both Strouhal (1878) and Rayleigh (1896) in the 19th century. Theoretical analysis was developed by Curle (1955) who demonstrated that the sound is a dipole-type source, generated principally by the unsteady pressure interaction with the cylinder surface, as summarized more recently by Powell (1990). The effect of externally imposed sound on the flow over a single cylinder has been reported by Blevins (1985), who concluded that sound levels greater than 130 dB resulted in a reduction in the small variation of the vortex-shedding frequency. The noise generated by impingement on a body in the wake of vortex dominated flow has been reported by, for example, Ziada and Rockwell (1982) for a wedge downstream of a jet, and sound generated by flows over cavities and slots has been investigated by Bruggeman et al. (1991). In many of these cases, there is feedback interaction between the velocity and pressure fields, with the potential for phase locking resulting in increased noise generation as proposed by Powell (1953).

The study of two tandem cylinders (i.e., one behind the other) in a cross-flow provides a useful vehicle to develop an understanding of the mechanisms of flow/acoustic interactions. The characteristics of the flow around two cylinders has been extensively reviewed by Zdravkovich (1977) who has shown that vortex formation in the inter-cylindrical space is

E-mail address: john.fitzpatrick@tcd.ie (J.A. Fitzpatrick).

0889-9746/03/$ - see front matter
PII: S0889-9746(02)00091-9

only present when the nondimensional spacing is greater than approximately four diameters. Ljungkrona et al. (1991) have reported a series of experiments on flow interactions for tandem cylinders and demonstrated that there was no significant vortex action between the cylinders for nondimensional spacing of less than 3.4–3.8. More recently, Mahir and Rockwell (1996) have reported on an extensive study of the effect of vibration on the flow around two cylinders in tandem. Their work focused on the ability of the vibration to "lock on" to the vortex shedding systems, but indicated an absence of vortex shedding for small inter-cylinder spacing.

Nonlinear interactions in the free shear layer bounding a vortex street have been studied both theoretically and experimentally. The instability of a shear layer under the influence of vorticity and its capacity to produce harmonics due to nonlinear interactions has been predicted by Stuart (1967) and has been observed by Ziada and Rockwell (1982) for a jet impinging on a wedge. A number of methods have been proposed for analysis of nonlinear interactions in flows. The most common has been the use of the bispectrum which seeks to determine the degree of quadratic interaction for a specific variable and between variables [e.g., Hajj et al. (1997)]. However, Fitzpatrick and Rice (1990) showed that, due to multiple interactions, it is difficult to obtain quantitative information from bispectral analysis and they proposed an alternative technique to investigate nonlinear interactions.

The objective of the present work was to conduct a systematic study of the flow and acoustic characteristics for two cylinders in tandem. In the first part of the paper, experimental results from a two-cylinder configuration are reported in detail and show that nonlinear interactions are present in the measurements. These nonlinear interactions are then examined using both the bispectral approach and a development of the spectral technique proposed by Rice and Fitzpatrick (1988). The objective is to identify the quadratic interactions in the unsteady velocity and between the unsteady velocity and the near-field pressure.

2. Experimental set-up and analysis

The experiments were performed in a low-speed tunnel the test-section of which was 300 mm × 300 mm and velocity range from 15 to 50 m/s. Two cylinders of 8 mm diameter and 100 mm long were mounted between two parallel plates so that the inter-cylinder spacing could be varied and the plates were supported in the test-section. A turbulence grid could be installed upstream of the test-section, so that the freestream turbulence levels could be increased from 1% to 10%. The tunnel velocity was monitored using a Pitot static tube. A TSI hot-film anemometer was used to measure the local flow characteristics and two B&K microphones type 4138 were used to monitor the fluctuating pressure, one mounted flush at the top of the tunnel (far field) and the other, with a nose cone, was used in the vicinity of the two cylinders (near field). Measurements with the hot film and the near-field microphone were obtained along the nominal free shear layer between the cylinders, for nondimensional inter-cylinder spacings (i.e., L/d) of 5.0, 4.0 and 3.0 without and with the turbulence grid installed. A schematic of the set-up and measurement positions is shown in Fig. 1. The near-field microphone was then used to map the noise field in the vicinity of the cylinders for each of these configurations at 40 m/s.

Data was logged using a PC-based acquisition system with suitable anti-aliasing filters. The analysis of the data was accomplished using MATLAB-based software to calculate auto-spectra, cross-spectra, bispectra and bicoherences for

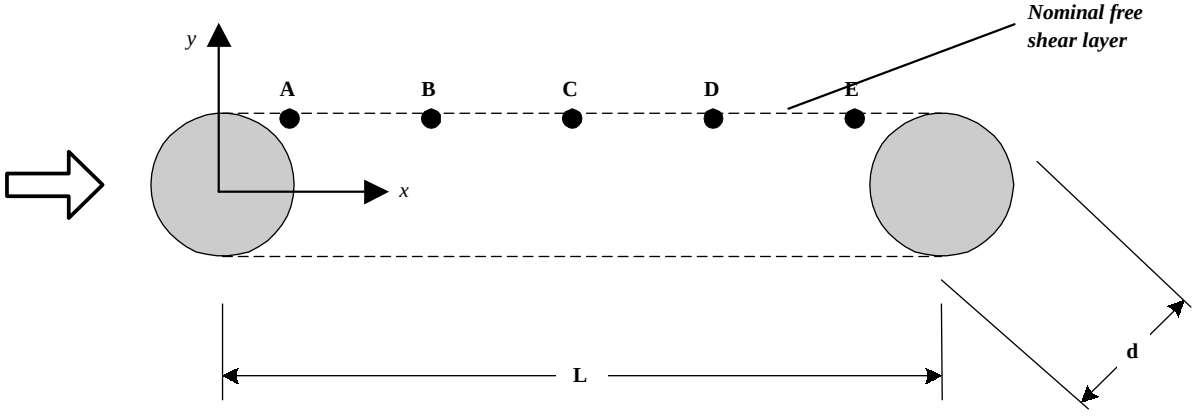

Fig. 1. Schematic of test layout.

the pressure and turbulence data. The anemometer data was linearized using a fifth-order polynomial before any spectral calculations were performed. Auto- and cross-spectra were calculated for 40 ensemble averages of 1024 data-points which had been sampled at 8 kHz. For the bispectra and bicoherence calculations, 256×256 points with 10 averages were used.

3. Test procedures and results

Experiments were conducted in which measurements were obtained using both the microphones and hot film anemometer to investigate the correlation between the pressure and the velocity fluctuations. The hot wire was positioned along the nominal free shear layer between the two cylinders, and simultaneous measurements were taken for different flow velocities and various inter-cylinder spacings. The turbulence screen was used upstream of the two cylinders to examine the effect of free-stream turbulence on the measurements of near-field pressure and turbulence. A preliminary series of tests was performed to ensure that the acoustic resonance frequencies of the tunnel, with a fundamental of 560 Hz, were not excited for the velocity range to be used.

3.1. *Configuration 1* ($L/d = 5$)

For this configuration, initial tests were performed at a series of flow velocities and measurements were obtained for the near-field noise and turbulence midway between the two cylinders ($x/d = 2.5$) and for the far-field noise at the tunnel wall. Fig. 2 shows the spectra from these measurements plotted as nondimensional frequency (Strouhal number). The Strouhal number for this configuration was found to be 0.18 (based on free-stream velocity) with turbulence levels at the measurement point along the nominal free shear layer of 7% and local velocity of 0.75 mainstream velocity. The

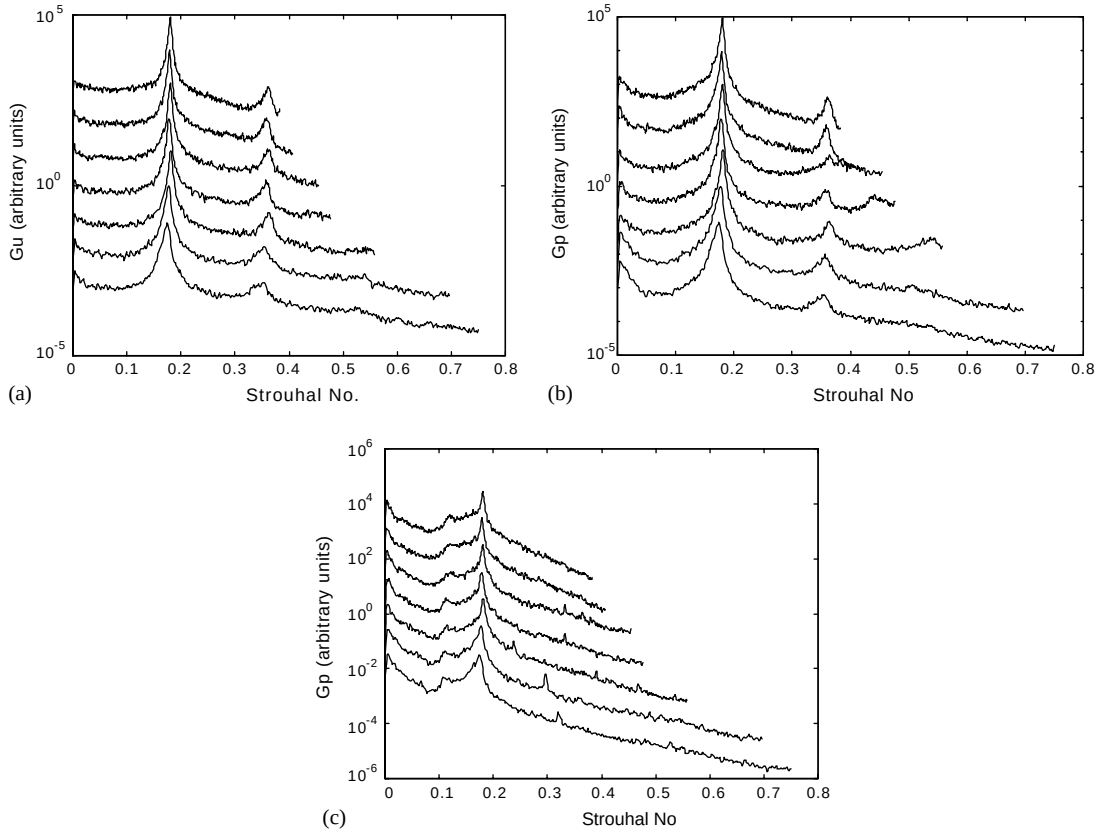

Fig. 2. Auto-spectra at C ($L/d = 5$): (a) turbulence spectra; (b) near-field pressure spectra; and (c) far-field pressure spectra.

sound pressure levels in the near field varied from 145 to 148 dB. The relative amplitude of the harmonic in the turbulence spectrum can be seen to be increasing with velocity. It can be seen that, whilst the near-field pressure spectrum clearly exhibits a peak at both the shedding frequency and the first harmonic, the latter is not discernible in the far field. The coherence between the hot wire and near-field microphone was greater than 0.96 at the fundamental frequency and varied from 0.3 to 0.6 for the first harmonic. The coherence between the hot wire and the far-field microphone was between 0.85 and 0.9 at the vortex-shedding frequency and it varied from 0 to 0.2 at the first harmonic, indicating that this is submerged in the tunnel noise. Similar results were found for the coherence between the near- and far-field microphones. Fig. 3 shows a plot of the near-field pressure level as a function of velocity.

Further tests were performed with the near-field microphone fixed at position C ($x/d = 2.5$), and the hot wire traversed along the nominal free shear layer at $x/d = 0.5$, 1.5, 2.5, 3.5 and 4.5 (i.e., A, B, C, D and E). Results for the turbulence and near-field pressure spectra were obtained for velocities of 26 and 40 m/s, with and without the turbulence grid installed upstream of the test-section. The results for 40 m/s are shown in Fig. 4 and the effect of the turbulence

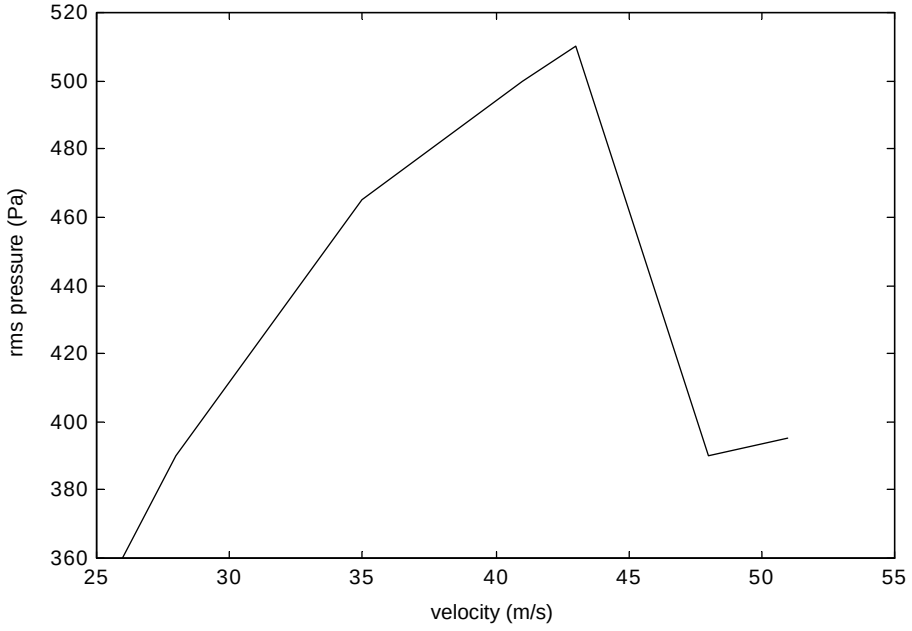

Fig. 3. RMS pressure at C ($L/d = 5$).

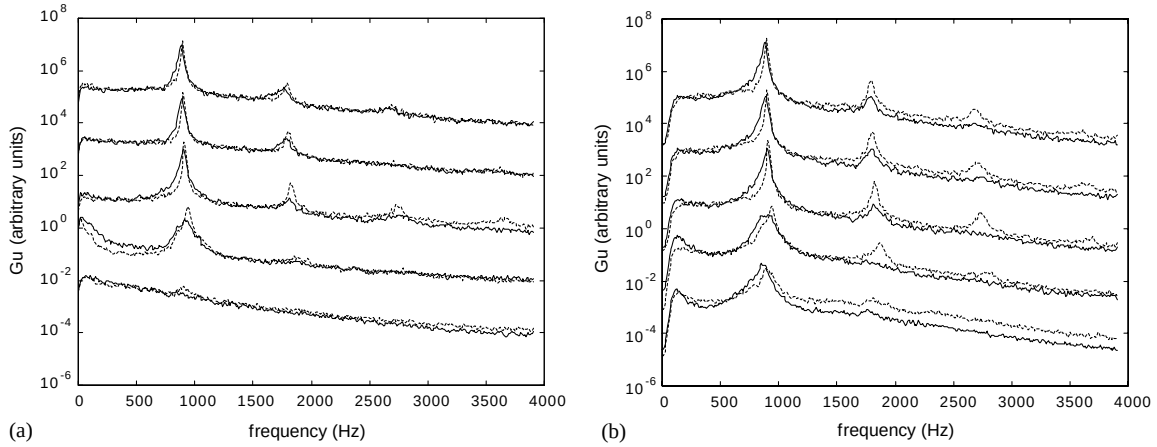

Fig. 4. Auto-spectra at 40 m/s ($L/d = 5$): (a) turbulence spectra; and (b) pressure spectra (- - -: no grid; —: grid) (from bottom: A, B, C, D, E).

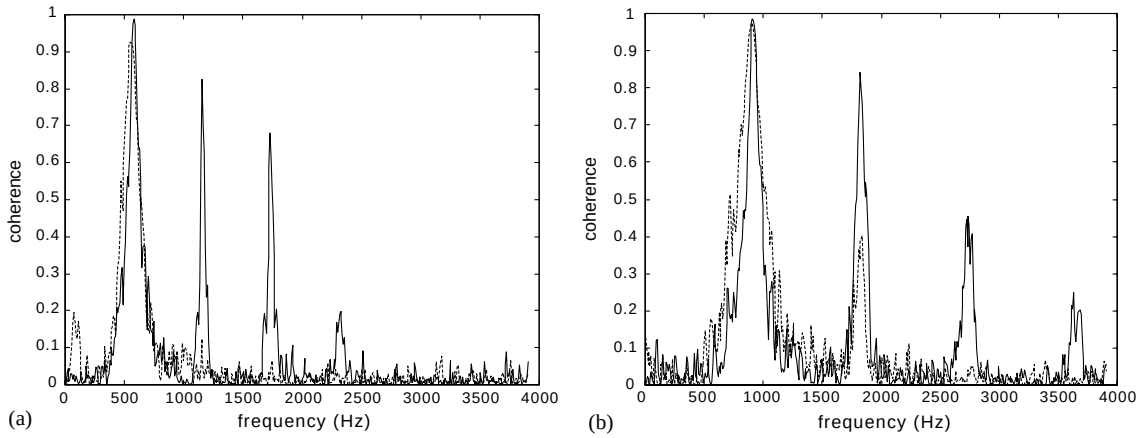

Fig. 5. Coherence at C ($L/d = 5$): (a) at 26 m/s; and (b) at 40 m/s (- - -: no grid; —: grid).

screen is quite marked, especially at position C where the vortex-shedding frequency together with three harmonics are clearly evident in the spectrum. From the near-field pressure spectra in Fig. 4(b), all measured at position C, the generation of harmonics along the free shear layer between the two cylinders has been inhibited by the location of the hot wire upstream of the measuring position. No harmonics were evident at 26 m/s without the grid, whereas a fundamental and three harmonics were observed when the turbulence grid was installed. It is clear that the generation of harmonics is a function of both the velocity and the turbulence levels of the mainstream flow. The coherence between the turbulence and near-field pressure for these measurements is shown in Fig. 5, and the effect of the turbulence is to enhance considerably the coherent noise generated at the harmonics of the vortex-shedding frequency by the incident turbulence.

The noise fields at the vortex-shedding frequency and the first harmonic around the two cylinders at a velocity of 40 m/s are shown in Fig. 6 for measurements without and with the turbulence screen. The noise at the vortex-shedding frequency for both nonturbulent and turbulent cases can be seen from Fig. 6(a) and (c) to be highest at the downstream cylinder with an increase of almost 5 dB for the latter. It is also noteworthy that a secondary peak source appears at midway between the two cylinders and that the extent of this is increased by a turbulent mainstream. At the first harmonic [Fig. 6(b) and (d)], the noise level is some 20 dB down on the vortex-shedding frequency and is radiating principally from the region just in front of the downstream cylinder. For the higher harmonics, discernible peaks were only observed close to the nominal free shear layer from the mid-point between the cylinders to the rear cylinder.

3.2. Configuration 2 (L/d=4)

With the inter-cylinder spacing (L/d) reduced to 4.0, hot film and near-field pressure measurements were obtained at the mid-point between the cylinders (i.e., $x/d = 2$) at velocities of 26 and 40 m/s. At the higher velocity the results are shown in Fig. 7(a) and (b). The first harmonic of the vortex-shedding frequency is beginning to appear and with the turbulence screen, two harmonics are observed with the first also clearly visible in the near-field pressure spectra. The coherence for these measurements is given Fig. 7(c) and only with the turbulence grid is there any significant coherence at the harmonics.

The effect of the grid on the noise field at the vortex-shedding frequency and first harmonic can be seen in Fig. 8. At the vortex-shedding frequency, the noise is principally radiated from the downstream cylinder with a 5 dB increase for the grid-generated turbulence. For this configuration, there is no evidence of a free stream dipole type source in the inter-cylinder gap such as was seen for configuration 1. At the first harmonic, the noise is again emanating from the free shear layer region in the latter half of the gap between the two cylinders.

3.3. Configuration 3 ($L/d = 3$)

For this configuration, tests were conducted at flow velocities of 26 and 40 m/s, without and with the turbulence screen. The results indicated that there was no discrete vortex action between the two cylinders for any of the measurements. However, for the near-field pressure spectra with incident turbulence, a broadband peak was clearly

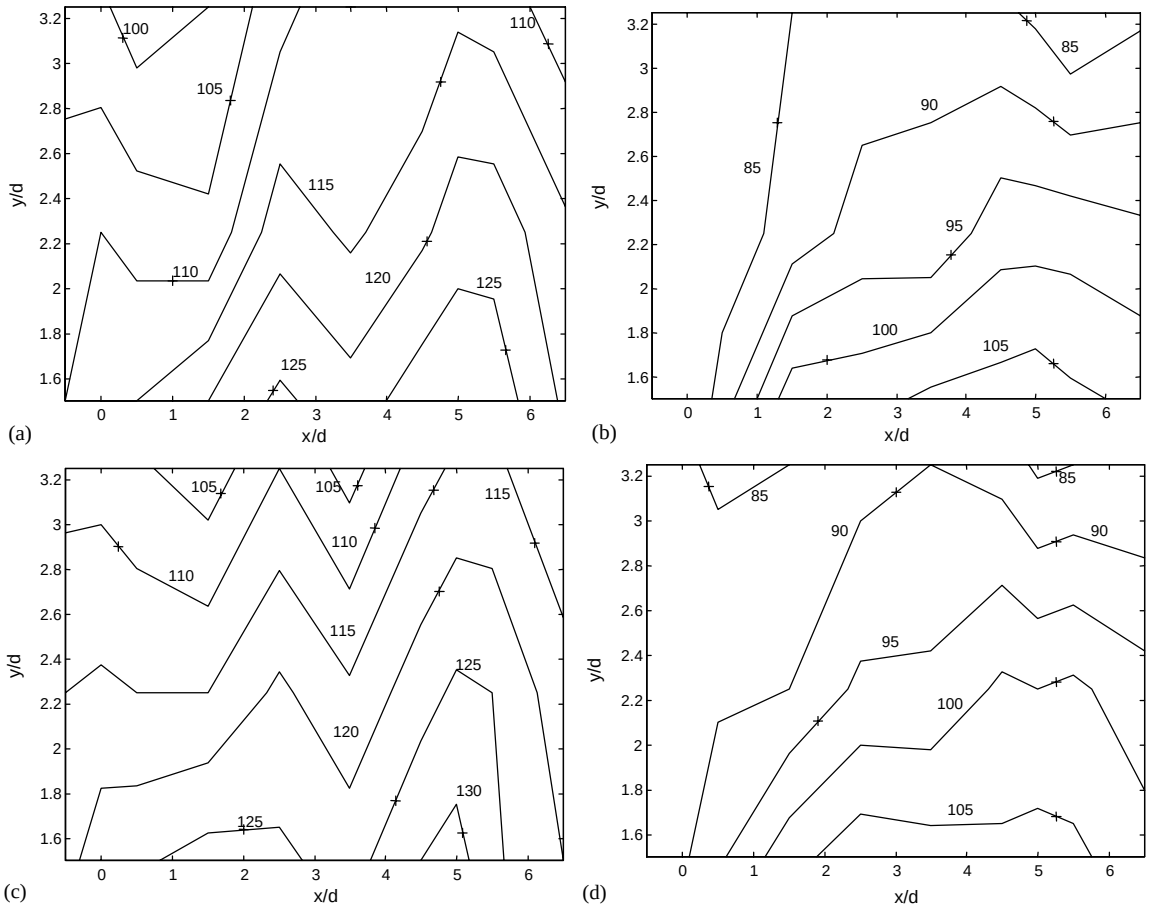

Fig. 6. Acoustic field at 40 m/s ($L/d = 5$): (a) vortex frequency (no grid); (b) first harmonic (no grid); (c) vortex frequency (with grid); and (d) first harmonic (with grid).

evident. It is possible that this peak was due either to turbulent buffeting or to vorticity action in the wake of the downstream cylinder, but there was insufficient evidence to justify this although the coherence between the turbulence and the pressure showed some signs of interdependence at the frequencies of interest.

4. Discussion of results

The results for configurations 1 and 2 show clearly that noise is generated at the vortex-shedding frequency and at a number of harmonics. For configuration 3, as no discrete vortex shedding was observed, the potential for noise generation is reduced. For the first two cases where vortex shedding was observed, the potential for feedback for two cylinders in cross-flow can be examined by considering the generation by vorticity shedding of a fluctuating pressure at the upstream cylinder. This disturbance is convected downstream, where it impinges on the downstream cylinder. This impingement then radiates upstream at the local relative velocity of sound and causes a further fluctuating pressure on the upstream cylinder. If this is in phase with the original unsteady pressure fluctuation, then positive feedback occurs and there is potential for enhanced noise generation. From Fig. 3, it can be seen that there is an increase in the noise generated for two cylinders spaced at $L/d = 5$ over the velocity range 35–45 m/s. This increase corresponds with the velocity range expected for possible phase locked acoustic feedback in low-speed flows as proposed by Powell (1953) using the relationship

$$L/\Lambda + L/\lambda = n + p,$$

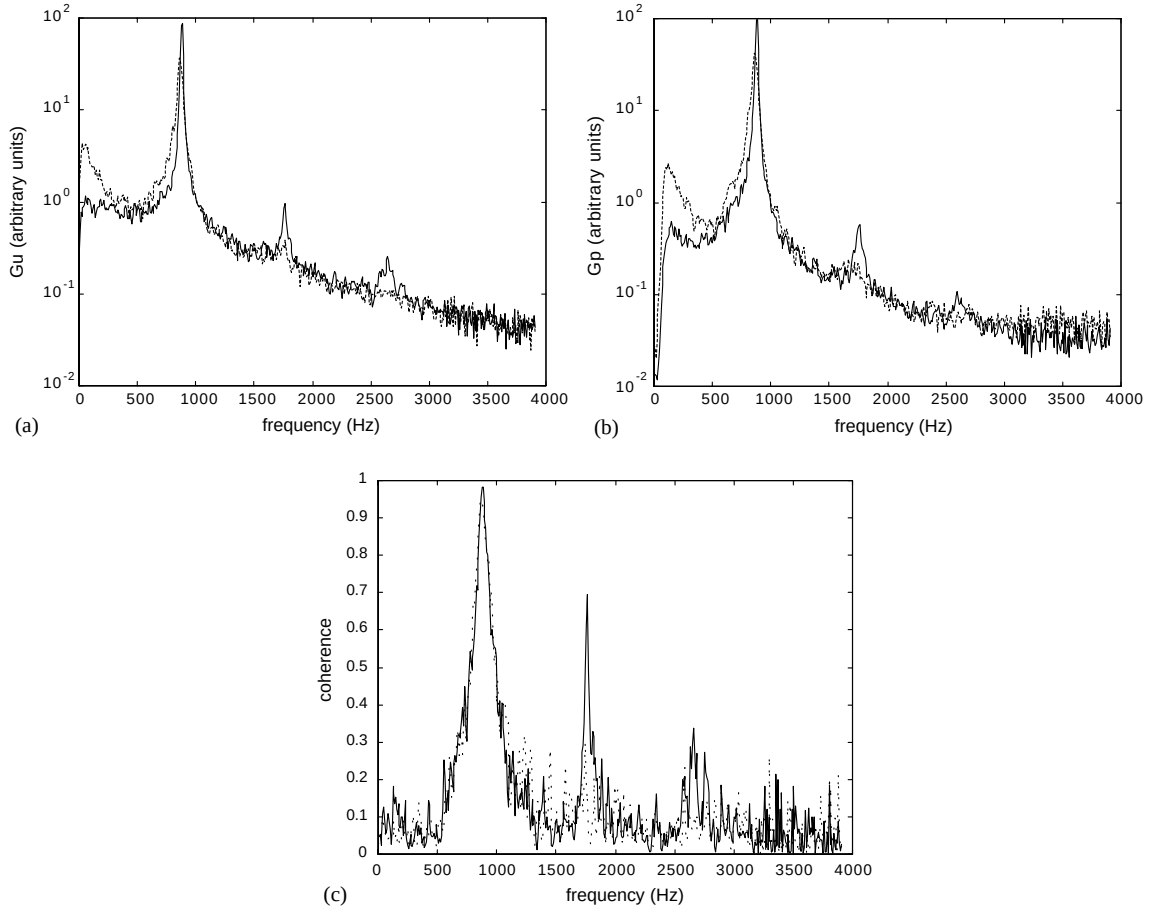

Fig. 7. Auto-spectra and coherence at 40 m/s ($L/d = 4$) : (a) turbulence spectra; (b) pressure spectra; and (c) coherence (- - -: no grid; —: grid).

where L is the separation distance and Λ and λ the convection and propagation wavelengths, respectively, with n an integer. The value for p was originally proposed by Powell (1953) as 1/4, but different values have been suggested by other authors [e.g., Kwon (1996)]. For these results, the value of 1/4 together with a Strouhal number of 0.18 suggests a critical velocity range around 40 m/s as has been observed. For configuration 2 with $L/d = 4$, the critical velocities would be higher than those reported here, so a phase locked condition would not be expected.

The effect of turbulence is clearly evident in both the sound levels generated and the capacity of the set-up to generate harmonics. It is obvious that incident turbulence increases the sound generated and enhances the nonlinear interactions giving rise to harmonics as was observed for both configurations 1 and 2. The results show clearly that the generation of harmonics is dependent on flow velocity, incident turbulence and, perhaps, the capacity of a system for feedback.

5. Nonlinear interactions

In most fluid flow systems, nonlinearity arises from velocity-product terms in the governing equations which give rise to quadratic interactions. In order to investigate this mechanism as a potential source for harmonic generation in wake flows giving rise to pressure fluctuations, there are two approaches available which attempt to identify quadratic-type interactions. The first of these is based on multi-spectral frequency domain analysis and the second seeks to identify the interactions by a time–frequency domain analysis.

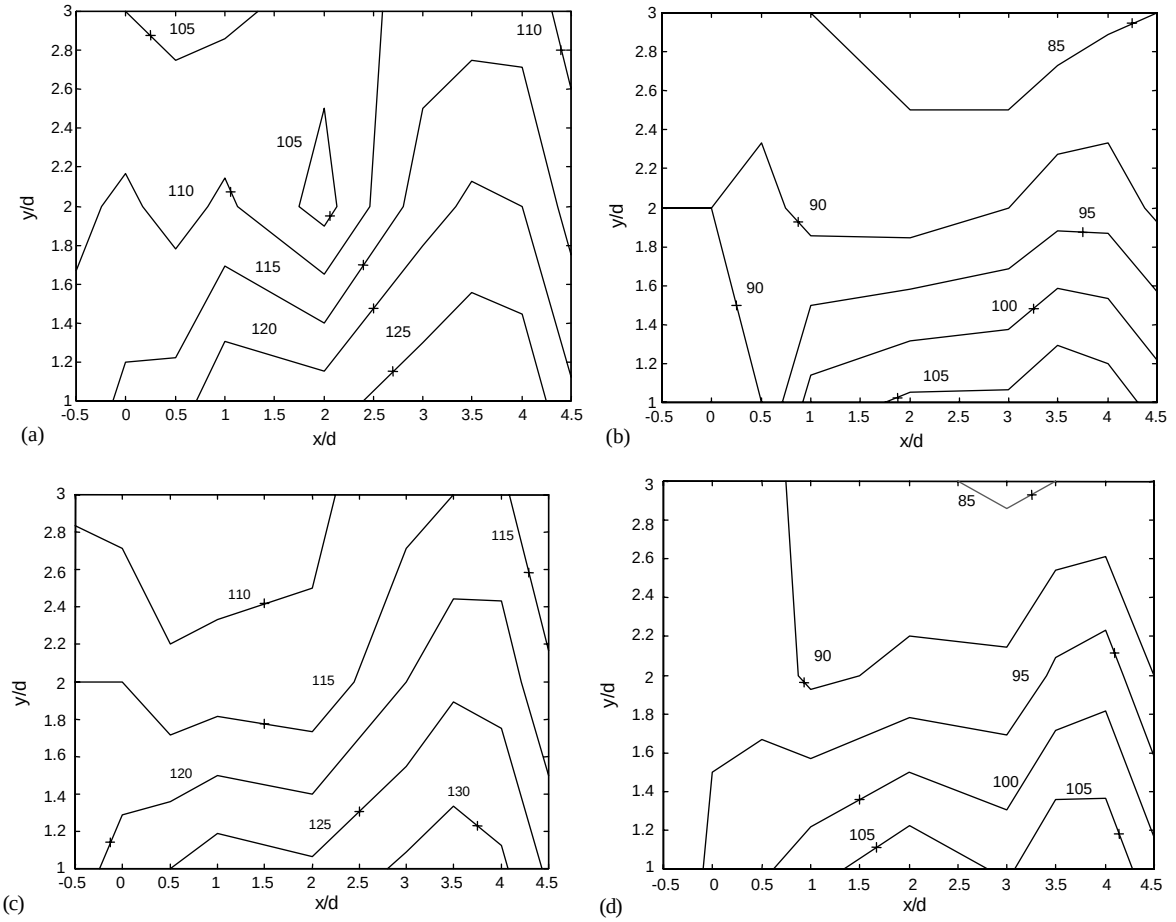

Fig. 8. Acoustic field at 40 m/s ($L/d = 4$) : (a) vortex frequency (no grid); (b) first harmonic (no grid); (c) vortex frequency (with grid); and (d) first harmonic (with grid).

5.1. Bispectral analysis

Bispectral analysis seeks to determine the element of quadratic coupling in a process. The auto-bispectrum of the unsteady velocity, $u'(t)$ is given by

$$B_{uu}(f_1,f_2) = E\langle (U^*(f_1)U^*(f_2)U(f_1+f_2)\rangle,$$

where $E\langle\ \rangle$ is the normal expectation operator and $U(f)$ is the finite Fourier transform of $u'(t)$. This can be shown to be zero for a Gaussian process and can be expected to be nonzero when there have been quadratic interactions in the development of $u(t)$. Thus, the bispectrum seeks to identify interactions at f_1 and f_2 which give rise to a third frequency f_3 which is the sum of the original frequencies. In many cases, the normalized version of the auto-bispectrum termed the auto-bicoherence is used and this is defined as

$$b^2(f_1,f_2) = [B_{uu}(f_1,f_2)][B^*_{uu}(f_1,f_2)]/E\langle [U(f_1)U(f_2)]^2\rangle E\langle [U(f_1+f_2)]^2\rangle.$$

This is equivalent to the coherence function $\gamma^2(f)$ and is also bounded by zero and unity. It is, therefore, a measure of the degree of quadratic coupling in a signal at two frequencies f_1 and f_2 which give rise to a third frequency f_3.

Where the quadratic coupling of the unsteady velocity $u'(t)$ and the pressure $p(t)$ are of interest, then the cross-bispectrum is used and this is given as

$$B_{up}(f_1,f_2) = E\langle U^*(f_1)U^*(f_2)P(f_1+f_2)\rangle.$$

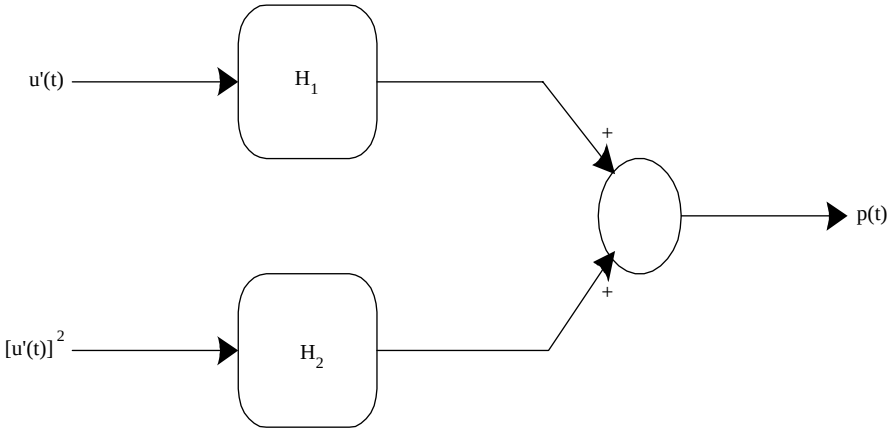

Fig. 9. Quadratic interaction model.

Again, this is a measure of how components at f_1 and f_2 in the turbulence spectrum give rise to response at f_3 in the pressure spectrum. With its associated cross-bicoherence, it can be used to identify quadratic effects in $u'(t)$ giving rise to $p(t)$. The symmetry properties of the cross-bispectrum and the cross-bicoherence have been detailed by Hajj et al. (1997). For the current paper, the main interest was in the frequency sum correlations, so only positive frequencies have been considered.

5.2. Quadratic time/frequency analysis

For this procedure, an additional variable, $[u'(t)]^2$ is formed and this can be used to determine the degree of quadratic interaction in $u'(t)$ and the degree of quadratic correlation between $u'(t)$ and $p(t)$. Consider the schematic shown in Fig. 9. Here, the system is represented as two inputs and an output. The inputs are considered as the turbulent velocity and the square of this, and the output is the pressure. Thus, linear source terms are governed by the relationship between $u'(t)$ and the output, and quadratic sources are determined from the relationship between $[u'(t)]^2$ and the output. Not only can the degree of correlation or coherence with the pressure be determined for both the "linear" and "nonlinear" elements using the technique, but the degree of "self–self" interaction in the velocity can also be quantified. For the latter, the correlation between $u'(t)$ and $[u'(t)]^2$, termed the quadratic coherence $q^2(f)$, indicates the degree of quadratic interaction present in the velocity data. In addition, the contribution of the linear and nonlinear terms to the pressure can readily be determined using conditioned spectral analysis which eliminates any correlation between u' and u'^2. The degree of correlation between the uncorrelated "inputs" and the conditioned output is then assessed using a partial coherence function in the same manner one uses a coherence function to assess the degree of interdependence between two variables. The procedures have been given in detail by Bendat and Piersol (1980) and applied to nonlinear systems by Rice and Fitzpatrick (1988).

6. Nonlinear analysis

From the turbulence spectra without and with the grid at 40 m/s for measurement positions B, C, D and E, harmonics in the spectrum were observed as the probe moved towards the downstream cylinder, and it was found that the inclusion of a turbulence grid enhanced considerably the strength of the harmonics at positions B, C and D with up the third harmonic (i.e., $4\times$ vortex frequency) evident at position C. The spectra at 26 m/s also showed clear evidence of harmonic development along the nominal free shear layer and, again, the results from position C exhibited the strongest harmonic response. Thus, the data clearly exhibits the characteristics of quadratic interaction and the suitability of the techniques for identifying these nonlinear interactions outlined in Section 5 can be investigated. The appearance of harmonics of the vortex-shedding frequency is most evident at 40 m/s with the turbulence grid so the data from this test was used to examine the effectiveness of the nonlinear identification procedures. The vortex-shedding frequency for the results to be analysed was 940 Hz.

6.1. Turbulent quadratic interactions

In the first instance, the bispectral approach was applied to the velocity data. From the auto-bispectra shown in Fig. 10, the symmetry in the auto-bispectrum is readily observed and a number of observations can be made. At position A as the shear layer separates from the upstream cylinder, there is some evidence in Fig. 10(a) of quadratic interaction at low frequency. Just downstream of this, at position B, there is significant interaction evident, with the auto-bispectrum in Fig. 10(b) exhibiting both sum and difference frequency activity, the former readily attributed to quadratic interactions whereas the latter is most likely a consequence of the variability of the vortex-shedding frequency. At position C [Fig. 10(c)], quadratic interactions giving rise to a doubling of frequency are dominant, whilst further downstream, at D and E, there is substantial additional activity showing that other frequencies which sum to 950 Hz are active. Thus, the results indicate that the degree of quadratic interaction is increasing along the shear layer towards the downstream cylinder. The auto-bicoherences given in Fig. 11 enable the degree of self/self nonlinear interaction to be quantified. The auto-bicoherence shows a low level of interaction at position A with clear peaks at the vortex-shedding frequency for positions B–E, with maxima of 0.08, 0.15, 0.08 and 0.075, respectively.

For the quadratic model, the analysis proceeds as described in Section 5.2 and results using this approach are presented in Fig. 12 as coherence, amplitude and phase so that the first identifies the degree of quadratic interaction and the second and third the magnitude and phase of this interaction, and so amplification can potentially be quantified. The results show how the interactions grow along the shear layer with little coherent interaction evident at position A

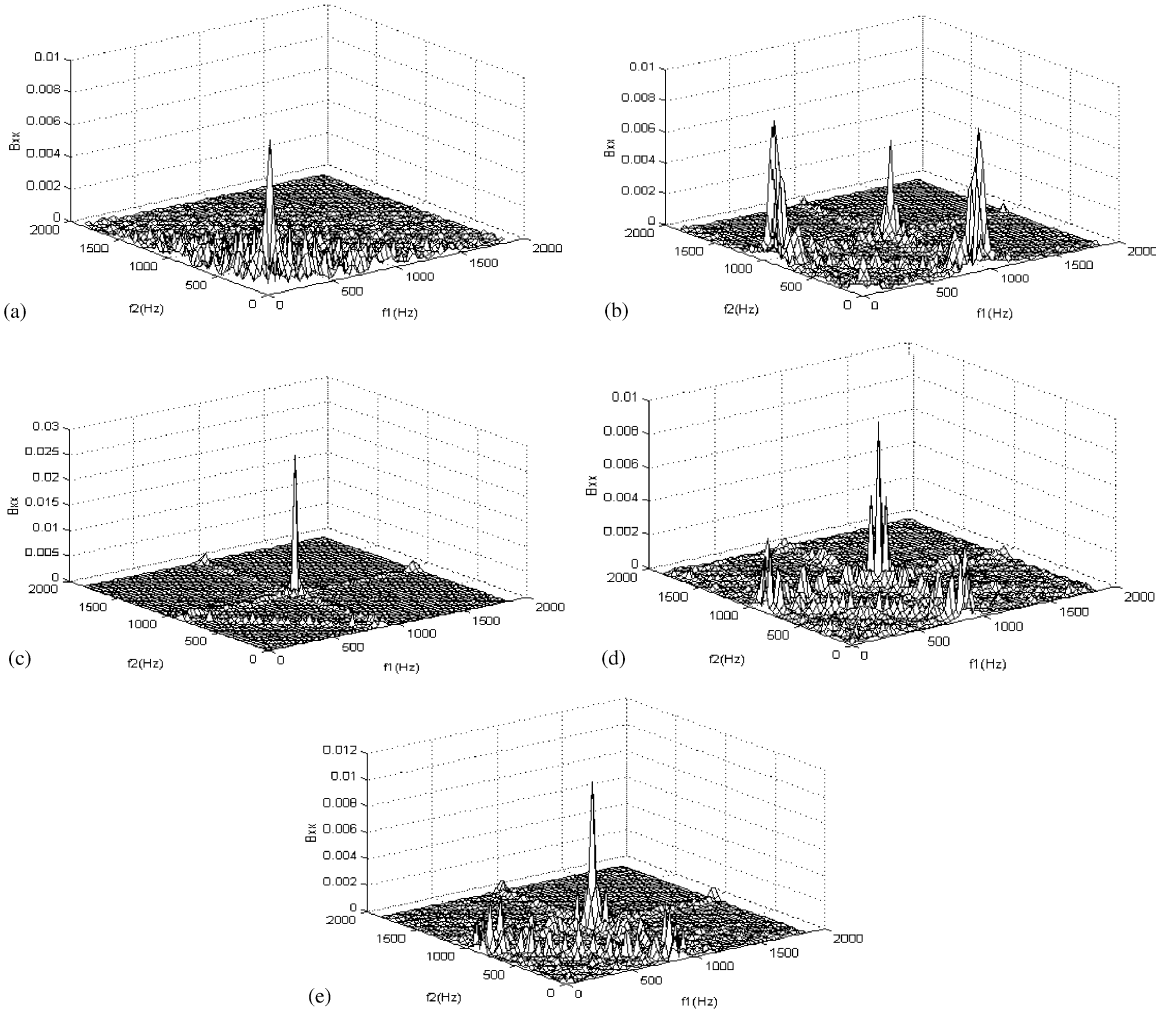

Fig. 10. Turbulence auto-bispectra at 40 m/s ($L/d = 5$): (a) at A; (b) at B; (c) at C; (d) at D; and (e) at E.

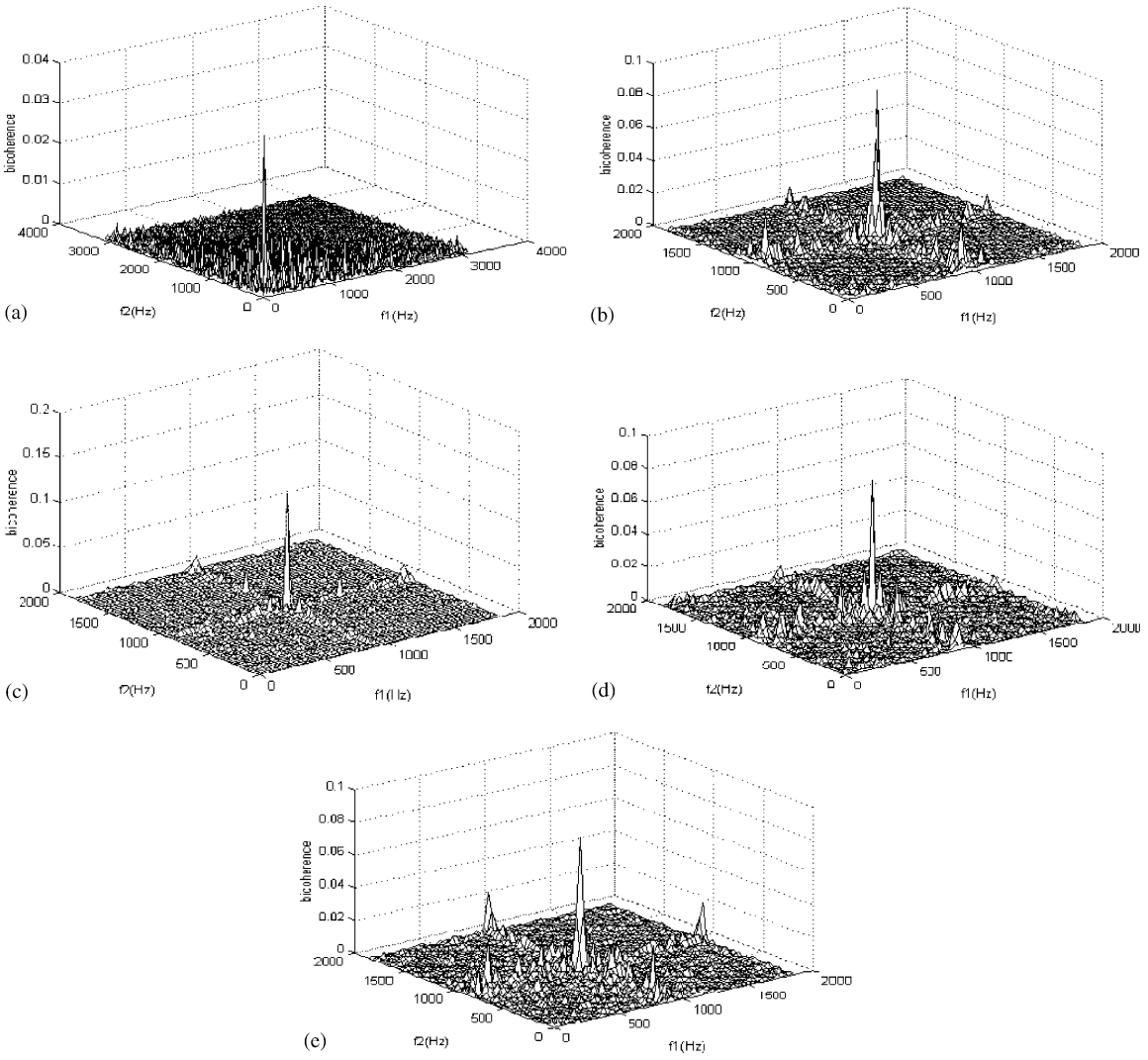

Fig. 11. Turbulence auto-bicoherence at 40 m/s ($L/d = 5$): (a) at A; (b) at B; (c) at C; (d) at D; and (e) at E.

and an increase in coherence as the measurement moves downstream, with strong interactions at the vortex-shedding frequency and the first harmonic (i.e., $2f_v$) with evidence of interactions at the second harmonic for position C. Unlike the bispectral approach, the quadratic interaction model can readily quantify the frequency response function between $u'(t)$ and $[u'(t)]^2$ so that the nonlinear nature of the evolution of the turbulence spectrum can be examined. At position A, there was no significant peak in the turbulence spectrum and from Fig. 12(a), it can be seen that the relationship between $u'(t)$ and $[u'(t)]^2$ is 0.5 as might be expected. For positions B, C, D and E, there is amplification between $u'(t)$ and $[u'(t)]^2$ at the first harmonic and a change in the phase relationship at this frequency from in phase at position B to out of phase at C and D, and in phase again at E. This implies that the nonlinear interactions are likely to be driven by a feedback mechanism resulting from the two cylinder configuration. It is also of interest to note that the degree of quadratic interaction is reduced as the flow approaches the downstream cylinder.

6.2. Turbulent/pressure interactions

The interaction between the turbulence monitored along the free shear layer and the unsteady pressure was then investigated using both the cross-bispectrum and the quadratic interaction model approaches. As the most significant

nonlinear interactions were observed at position C with the turbulence grid, the results for near-field pressure at this position were used together with turbulence measurements at A and C.

In the first instance, the cross-bicoherences between $u'(t)$ and $p(t)$ were found to show evidence of quadratic interaction and the results for 40 m/s with the turbulence grid are shown in Fig. 13 for positions A and C. At A there is no quadratic interaction evident, whereas at C it is clear that there is significant quadratic interaction between the velocity and the pressure. However, since it has been shown in the previous section that the auto-bicoherence of the turbulence is quite marked, it is difficult to use the cross-bispectral approach to quantify these interactions, as the cross-bispectrum will be contaminated by quadratically correlated components of $u'(t)$. Although a conditioning procedure has been suggested by Ritz et al. (1988), the implementation of this is complicated and the results are difficult to interpret.

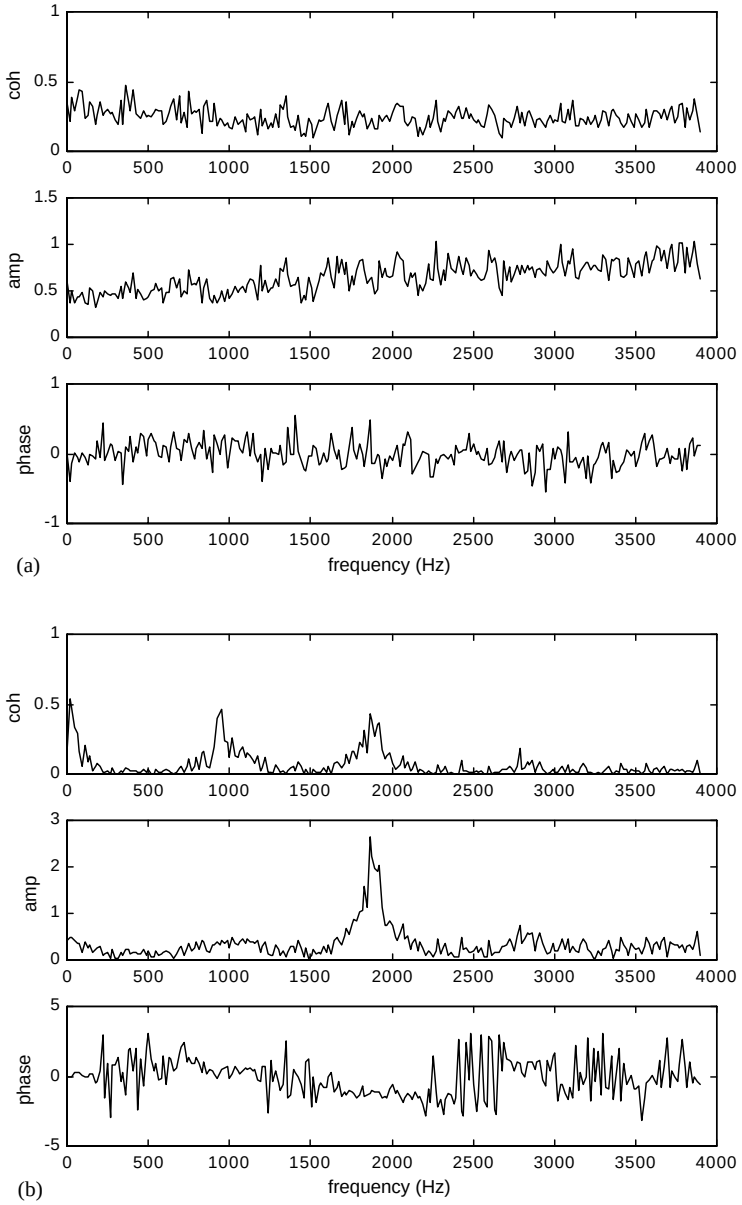

Fig. 12. Coherence, amplitude and phase at 40 m/s from quadratic model ($L/d = 5$): (a) position A; (b) position B; (c) position C; (d) position D; and (e) position E.

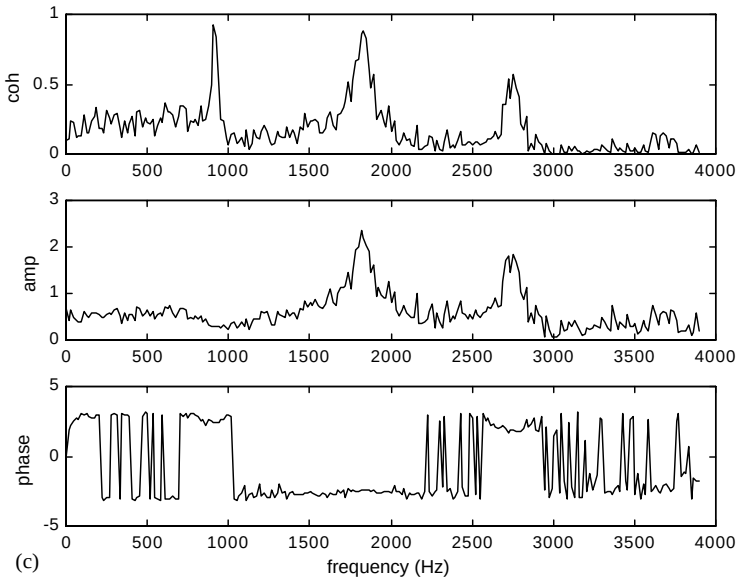

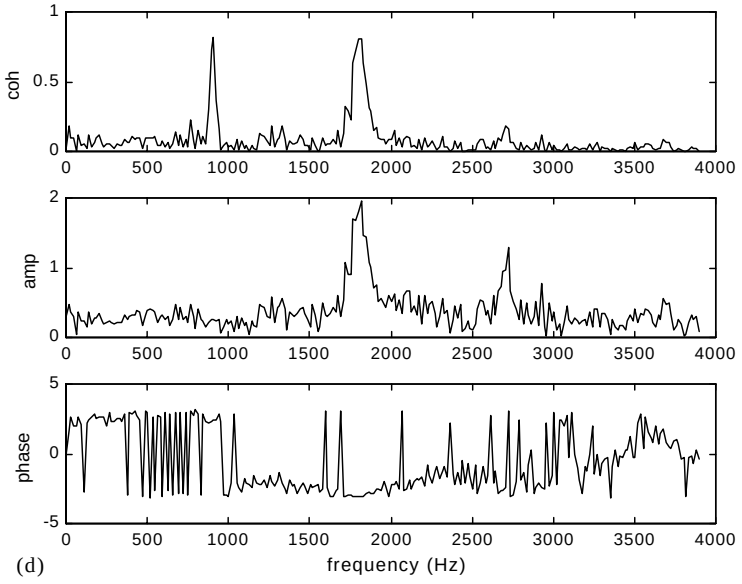

Fig. 12 (*continued*).

The quadratic modelling approach presents no such problem as the correlation between $u'(t)$ and $[u'(t)]^2$ is automatically catered for. The analysis proceeds as for a two input/output model where the mutual coherence between the inputs is eliminated using spectral conditioning [e.g. Bendat and Piersol (1980)] to obtain unbiased estimates of the two frequency response functions which determine the interaction between $u'(t)$ and $p(t)$ and between $[u'(t)]^2$ and $p(t)$. The partial and multiple coherences are shown in Fig. 14 for positions A and C. From Fig. 14(a), it can be seen that coherence only exists at the vortex-shedding frequency with no nonlinear interactions evident. This is to be expected as positioning of the hot wire at A was found to suppress the harmonics in the pressure field at C. At C, the coherence between $p(t)$ and $u'(t)$ can be seen to be >0.95 at the fundamental frequency, with a value of about 0.8 at the first harmonic and 0.3 at the second, whereas, for the partial coherence between $[u'(t)]^2$ and $p(t)$, there is coherence only at the first and second harmonics. For $u'(t)$, the coherence at the first and second harmonics arises because of the correlation between $u'(t)$ and $[u'(t)]^2$. This can be demonstrated by calculating the coherence between the $[u'(t)]^2$ and $p(t)$

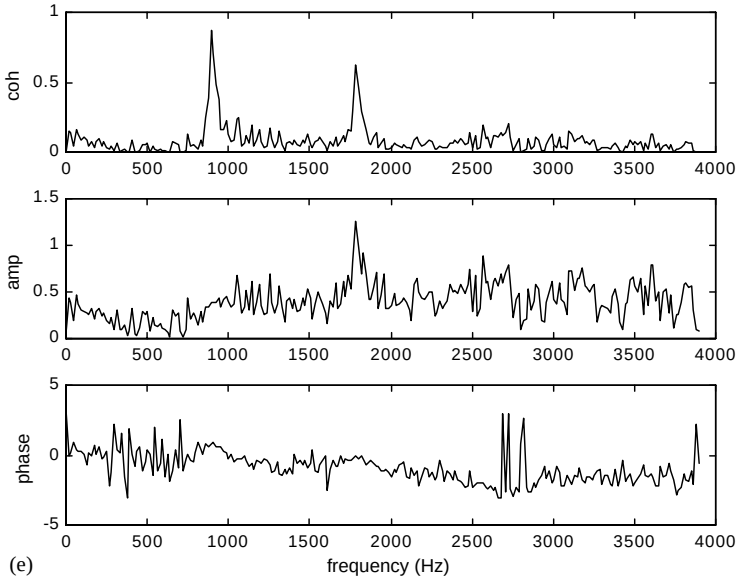

Fig. 12 (*continued*).

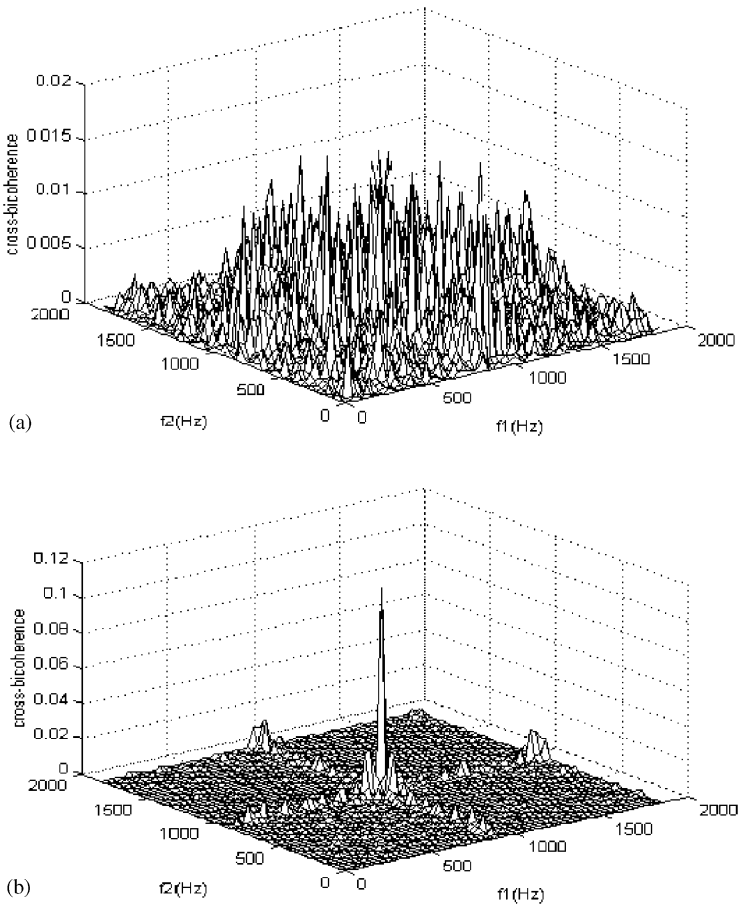

Fig. 13. Cross-bicoherence at 40 m/s ($L/d = 5$): (a) position A; and (b) position C.

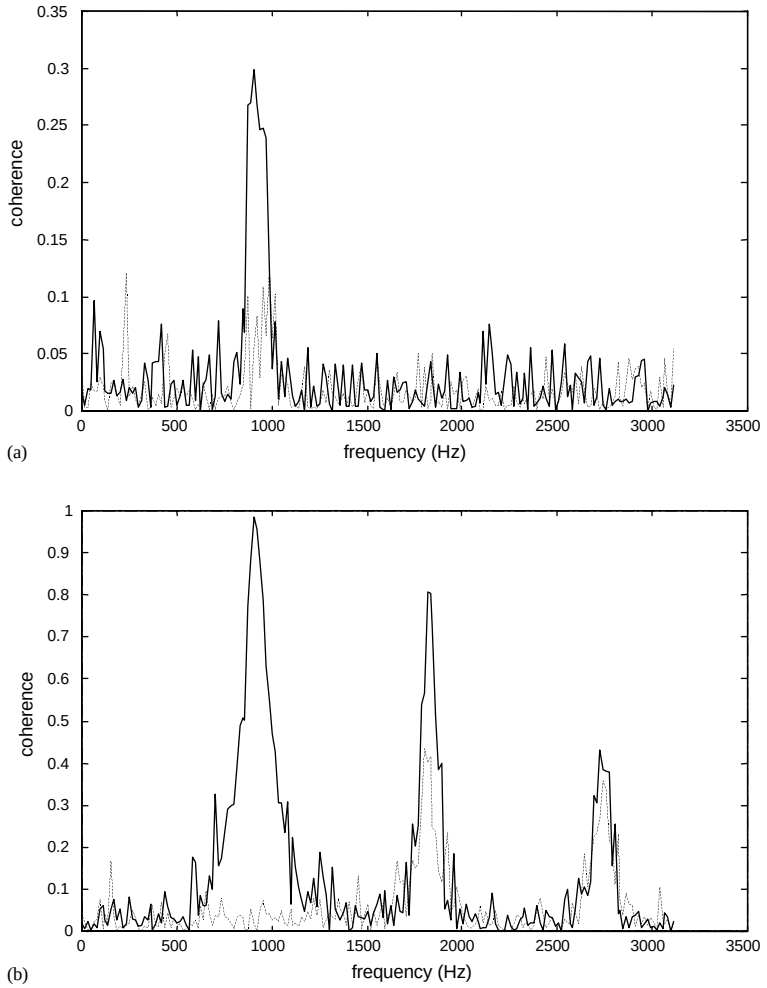

Fig. 14. Quadratic coherence at 40 m/s ($L/d = 5$) : (a) position A; and (b) position C (—: linear; - - -: nonlinear).

first, and then the partial coherence for $u'(t)$ and $p(t)$ exhibits correlation at the fundamental frequency only. The multiple coherence, which is the same regardless of the order of conditioning, shows that the proposed model accounts for all the output at the fundamental frequency, 80% of the pressure at the first harmonic and for 50% of the pressure at the second harmonic. The output at the fundamental frequency arises directly from the velocity fluctuations, whereas that at the first and second harmonics is a consequence of nonlinear interactions in the turbulent source terms. These can be quantified by determining the FRFs from the two-input model as shown in Fig. 15. From Fig. 15(a), the FRF between $p'(t)$ and $u'(t)$ gives a value of 24. with a phase of zero indicating that the value is positive. From Fig. 15(b), the FRF of $[u'(t)]^2$ and $p'(t)$ has a value of 0.7 at 1880 Hz again with a phase of zero.

6.3. Discussion

The nonlinear interactions in the developing shear layer between two cylinders have been examined using both a bispectral approach and a quadratic modelling technique. The use of the bicoherence has shown quadratic interactions along the shear layer and indicates that these increase in the downstream direction. The quadratic model not only identified these interactions but also quantified the degree of self–self interactions from the readily obtained FRF between $u'(t)$ and $[u'(t)]^2$. The coherence functions obtained using the quadratic model also show that there are likely to be additional quadratic interactions giving rise to the higher harmonics. In addition, the pressure fluctuations can influence the velocity fluctuations as demonstrated by Fitzpatrick and Valeau (1998). When a vortex impacts on the downstream cylinder and distorts, it gives rise to a pressure fluctuation at the fundamental frequency and the distortion

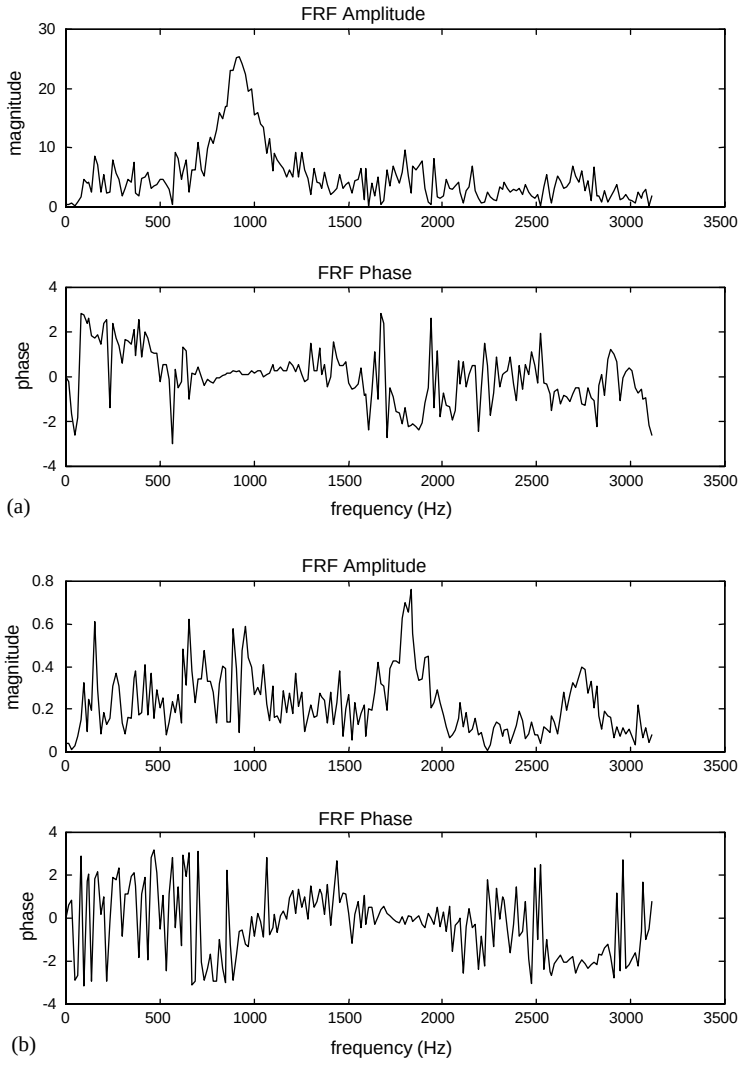

Fig. 15. Quadratic model FRFs at 40 m/s ($L/d = 5$): (a) linear path—position C; and (b) nonlinear path—position C.

generates harmonics which also propagate upstream. This condition can give rise to a phase locked condition which will enhance the vorticity strength and, as a consequence, increase the potential for nonlinear interactions. Thus, the source of noise at the second and higher harmonics of the vortex-shedding frequency in the two cylinder arrangement can be due to two effects: the first is the nonlinear distortion of the shear layer and the associated turbulent/turbulent interactions, and the second results from a pressure feedback which enhances the fundamental frequency and its harmonics. It is likely that both of these contribute to the characteristics observed at position C in the current configuration. The source of nonlinear interactions will only be resolved when the phase between the various contributing factors can be determined. Further development of the quadratic modelling approach should enable this phase relationship to be determined.

7. Conclusions

Detailed tests on the flow/acoustic behaviour of two cylinders in cross-flow have been reported and nonlinear interactions have been investigated using two methods of identification. From the results presented here, the following conclusions can be drawn.

(i) The frequency of the noise generated by two cylinders in tandem configuration with spacing of four diameters or more can be at the vortex-shedding frequency and its harmonics. For the configurations tested, only the fundamental and the first harmonic appear to radiate into the flow. The maximum noise levels were measured at the downstream cylinder for L/d of both 4 and 5. High levels were also obtained at the centre of the gap region for L/d of 5 (i.e., $x/d = 2.5$) indicating, again, the likelihood of feedback enhancing the strength of the vortex shedding process.

(ii) The auto-bicoherence can be used as a tool to identify the existence of quadratic interactions in turbulence data, especially when dominated by vorticity shedding processes. Cross-bispectral procedures have been used to show quadratic interactions of turbulence and pressure for the configuration tested.

(iii) The time/frequency modelling method has identified and quantified the quadratic interactions in the turbulence and determined the contributions of both linear and quadratic terms to the pressure. It has the potential to be developed as a powerful analysis tool for quantifying nonlinear phenomena in flow/structure/acoustic interactions.

Acknowledgements

The experiments reported in this paper were conducted at CIRA (Italian Aerospace Research Centre), Capua, Italy, where the author was a Senior Visiting Research Fellow. The author would like to acknowledge the assistance of Francesco Nitti and support of the European Commission TMR programme under Contract No. ERBCH-BICT941660.

References

Bendat, J.S., Piersol, A., 1980. Engineering Applications of Correlation and Spectral Analysis. Wiley Interscience, New York.

Belvins, R.D., Bressler, M.M., 1987. Acoustic resonance in heat exchanger tube bundles: Parts 1 and 2. ASME Journal of Pressure Vessel Technology 109, 275–288.

Blevins, R.D., 1985. The effect of sound on vortex shedding from cylinders. Journal of Sound and Vibration 161, 217–237.

Bruggeman, J.C., 1991, Self sustained aeroacoustic pulsations in gas transport systems: experimental study of the influence of closed side branches. Journal of Sound and Vibration 160.

Curle, N., 1955. The influence of boundaries upon aerodynamic sound. Proceedings of the Royal Society A 231, 505–514.

Fitzpatrick, J.A., 1985. The prediction of flow-induced noise in heat exchanger tube arrays. Journal of Sound and Vibration 99, 425–435.

Fitzpatrick, J.A., Rice, H.J., 1990. Equivalent time domain procedures for bispectral analysis. Journal of Sound and Vibration 137, 131–134.

Fitzpatrick, J.A., Valeau, V., 1998. Measurements of the spatial coherence of the flow around two cylinders. In Proceedings of 9th International Symposium on Application of Lasers in Fluid Mechanics, Lisbon, pp. 2071–2078.

Hajj, M.R., Miksad, R.W., Powers, E.J., 1997. Perspective: Measurements and analyses of nonlinear wave interactions with higher order spectral moments. ASME Journal of Fluids Engineering 119, 3–13.

Kwon, Y.-P., 1996. Phase-locking condition in the feedback loop of low-speed edge tones. Journal of the Acoustical Society of America 100, 3028–3032.

Ljungkrona, L., Norberg, Ch., Sunden, B., 1991. Free-stream turbulence and tube spacing effects on surface pressure fluctuations for two tubes in an in-line arrangement. Journal of Fluids and Structures 5, 701–727.

Mahir, N., Rockwell, D., 1996. Vortex shedding from a forced system of two cylinders. Part I: tandem arrangement. Journal of Fluids and Structures 10, 473–489.

Powell, A., 1953. On edge tones and associated phenomena. Acustica 3, 233–244.

Powell, A., 1990. Some aspects of aeroacoustics: from Rayleigh until today. ASME Journal of Vibrations and Acoustics 112, 145–159.

Rayleigh, L., 1896, The Theory of Sound, Vol. II. MacMillan & Co. Ltd., London.

Rice, H.J., Fitzpatrick, J.A., 1988. Spectral analysis of non-linear systems. Mechanical Systems and Signal Processing 2, 195–207.

Ritz, Ch.P., Powers, E.J, Miksad, R.W., Solis, R.S., 1988. Non-linear spectral dynamics of a transitioning flow. Physics of Fluids 31, 3577–3588.

Strouhal, V., 1878. Ueber eine besondre Art der Tonnerung. Annalen der Physik 5, 216–251.

Stuart, J.T., 1967. On finite amplitude oscillations in laminar mixing layers. Journal of Fluid Mechanics 29, 417–440.

Zdravkovich, M.M., 1977. Review of flow interference between two circular cylinders in various arrangements. ASME Journal of Fluids Engineering 99, 618–633.

Ziada, S., Oengören, A., 1989. On acoustical resonances in tube arrays: Parts 1 and 2. Journal of Fluids and Structures 3, 293–324.

Ziada, S., Rockwell, D., 1982. Oscillations of an unstable mixing layer impinging upon a wedge. Journal of Fluid Mechanics 124, 307–334.